Viana *et al. Biochar* (2024) 6:83
https://doi.org/10.1007/s42773-024-00371-w

Biochar

ORIGINAL RESEARCH

Open Access

Sugarcane straw biochar: effects of pyrolysis temperature on barite dissolution and Ba availability under flooded conditions

Douglas G. Viana[1,2], Matheus B. Soares[1,2], Luís Reynaldo F. Alleoni[1], Fernando B. Egreja Filho[3], Owen W. Duckworth[2] and Jussara Borges Regitano[1*]

Abstract

Reductive dissolution of barium (Ba) sulfate in wetland soils may increase Ba bioavailability in the environment, yet no information is available regarding Ba remediation using biochar. This study investigated the effectiveness of sugarcane (*Saccharum officinarum*) straw biochar pyrolyzed at 350 °C (BC350), 550 °C (BC550), and 750 °C (BC750) in inhibiting barite dissolution and, consequently, Ba availability in a soil artificially spiked with barite and flooded for 365 days. Increasing pyrolysis temperature alters the carbon structure, and increases dehydration and depolymerization, resulting in more stable biochar that releases less DOC (8.6-fold decrease from BC350 to BC750). Additionally, high-temperature biochar (BC750) had 1.7 times higher carbon (C) content, 2.4 times higher ash content, and a 13.1 times greater specific surface area (SSA) than low-temperature biochar (BC350). Amending soil with BC750 increased pH but did not promote reducing conditions, and thus did not promote barite dissolution. Conversely, greater DOC in low-temperature biochar, particularly BC350, favored reducing conditions and increased barite dissolution by 23%, with BC550 also showing an 18% increase. This enhancement led to a greater pool of Ba sorbed into more labile exchangeable sites. In summary, pyrolysis temperature affects biochar attributes, which in turn influences the soil geochemical environment and Ba speciation. Low-temperature biochar (BC350) shows potential as an amendment to increase the bioavailable Ba pool in assisted remediation programs, such as biochar-assisted phytoremediation.

Highlights

- Biochar pyrolysis temperature affected both redox potential and barite dissolution.
- BC750 mitigated barite dissolution while modifying exchangeable sorption sites.
- DOC release from low temperature biochar promoted barite reductive dissolution.
- BC350 may enhance biochar-mediated phytoremediation applications.

Keywords Anoxic soil, Wetlands, Ba remediation, Redox potential, DRIFT

*Correspondence:
Jussara Borges Regitano
regitano@usp.br
Full list of author information is available at the end of the article

Springer

© The Author(s) 2024. **Open Access** This article is licensed under a Creative Commons Attribution 4.0 International License, which permits use, sharing, adaptation, distribution and reproduction in any medium or format, as long as you give appropriate credit to the original author(s) and the source, provide a link to the Creative Commons licence, and indicate if changes were made. The images or other third party material in this article are included in the article's Creative Commons licence, unless indicated otherwise in a credit line to the material. If material is not included in the article's Creative Commons licence and your intended use is not permitted by statutory regulation or exceeds the permitted use, you will need to obtain permission directly from the copyright holder. To view a copy of this licence, visit http://creativecommons.org/licenses/by/4.0/.

Graphical Abstract

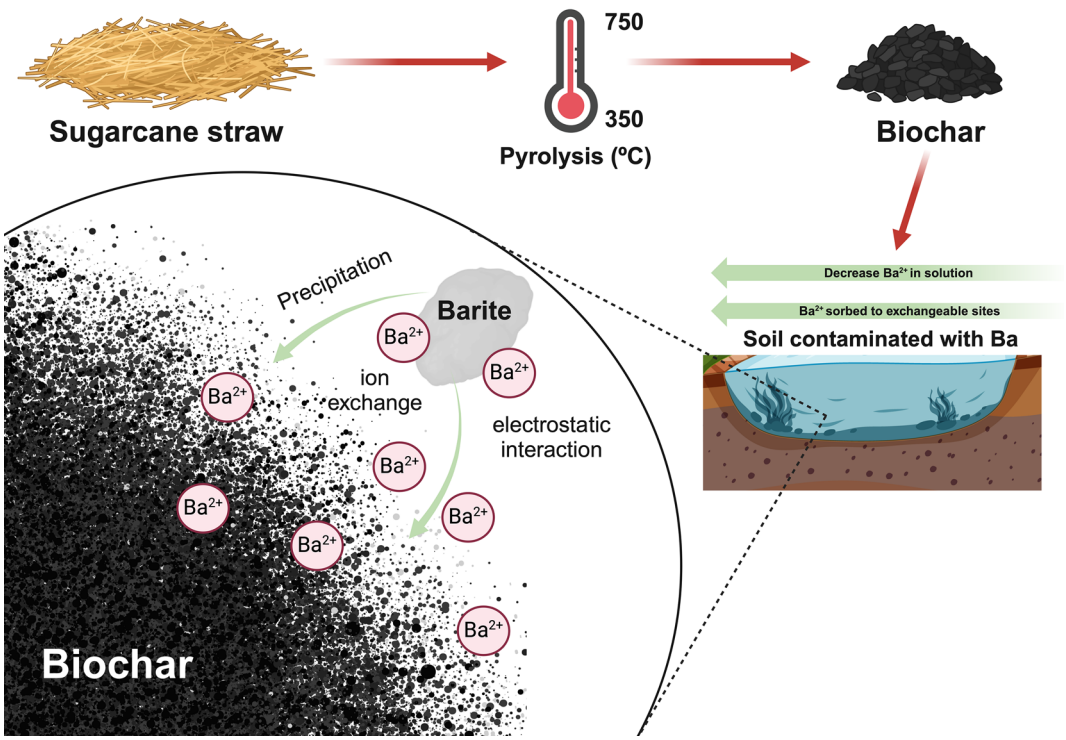

1 Background

Human exposure to barium (Ba), a potentially toxic element typically found in the environment as a divalent cation, can occur through contaminated food and water, inhalation, and skin contact (Peana et al. 2021). Its ingestion can lead to various health issues, including acute hypertension, hypokalemia, diarrhea, and cardiac arrhythmia (Dallas and Williams 2011). In plants, Ba excess can significantly affect their metabolic activity, leading to oxidative stress (de Souza Cardoso and Monteiro 2021; Bouslimi et al. 2021). In animals, it can result in hypokalemic paralysis because Ba^{2+} can act as a physiological antagonist to K^{+} (Tao et al. 2016; Willems et al. 2023). Therefore, the United States Environmental Protection Agency (USEPA) has set the Maximum Contaminant Level (MCL) at 2000 μg L^{-1} for Ba in drinking water (USEPA 2002). Similarly, soil screening limits are 330 mg kg^{-1} in the US (USEPA 2005) and 300 mg kg^{-1} in Brazil (CONAMA 2009).

Anthropogenic activities have significantly increased Ba pollution, and thus the potential for human exposure, through widespread use in multiple industrial sectors, such as explosives, cosmetics, fire extinguishers, and nanoparticles (Chałupnik et al. 2019; Peana et al. 2021; Konduru et al. 2014). Major anthropogenic sources of Ba in the environment include ore mining and refining, Ba salt manufacturing, and oil spills (Lamb et al. 2013; Choudhury and Cary 2001). In the petrochemical sector, barite ($BaSO_4$) is used to increase the hydrostatic pressure of drilling mud (Lamb et al. 2013). Latin American nations, such as Brazil, Venezuela, Mexico, Ecuador, Argentina, and Colombia, host ~ 20% of the world's oil reserves, producing ~ 8 million barrels per day (~ 10% of global demand), (Solano-Rodríguez et al. 2021), thereby escalating the risk of environmental contamination in this region.

Soil pH and redox potential (Eh) dictate Ba fate in soils (Rinklebe et al. 2016; Kravchenko et al. 2014). In oxic conditions (Eh > 350 mV; Otero et al. 2009), barite poses a minimal environmental threat due to its low solubility. However, wetland soils and waters near oil extraction sites often have large Ba concentrations during prolonged anoxia (Carvalho et al. 2019). Under these anaerobic conditions (Eh < 100 mV; Otero et al. 2009), sulfate (SO_4^{2-}) reduction to sulfide (S^{2-}) species can lead to reductive barite dissolution with a concomitant increase in Ba^{2+} bioavailability (Viana et al. 2021a). Generally, Ba solubility rises as pH decreases (Kravchenko et al. 2014),

but it depends on the Ba solid controlling solubility. For instance, $BaCl_2$ is less sensitive to pH changes than $BaSO_4$ or $BaCO_3$ (Tang and Johannesson 2010).

Assessing ways to remediate Ba contamination is crucial, especially in anoxic environments. One promising method involves using eco-friendly wastes to trap potentially toxic elements (PTEs) in wetlands (Li et al. 2016). Biochar shows potential for remediating Ba and other pollutants, such as antimony (Hua et al. 2021), arsenic (Mukherjee et al. 2021), cadmium (Chen et al. 2022), lead (Qian et al. 2022), and mercury (Shen et al. 2021), from water and soil at a low cost (Li et al. 2016; Vithanage et al. 2016). Brazil, the largest sugarcane (*Saccharum officinarum*) producer globally, yields about 643 million tons annually (Martíni et al. 2020), mostly without straw burning. This residue can be converted into biochar for various beneficial uses, including remediation (Yuan et al. 2011; Zama et al. 2017; Wang and Wang 2019; Younis et al. 2020). However, biochar's effectiveness in remediation systems depends on feedstock biomass and processing method (i.e., pyrolysis conditions) (Wang and Wang 2019).

Factors such as pyrolysis temperature influence biochar properties and thus its suitability for environmental remediation (Ding et al. 2014). Higher pyrolysis temperatures often enhance surface area, pH, volatile material, and carbonized fractions, but decrease cation exchange capacity (CEC) and number of surface reactive functional groups (Tomczyk et al. 2020). Additionally, biochar-derived organic matter can act either as an electron donor or acceptor (Yuan et al. 2017) and, consequently, impact the redox-dependent mobility of PTEs during soil flooding (Yang et al. 2021; Rinklebe et al. 2020). Despite its potential and the complicated impacts of preparation on its properties, research on the effects of biochar on contaminant mobility in flooded soils remains limited (Rinklebe et al. 2020; El-Naggar et al. 2018).

The primary objective of this study was to assess how biochar pyrolysis temperature impacts Ba availability in flooded soil spiked with barite to better understand its potential use in soil remediation. Sugarcane straw was pyrolyzed at temperatures of 350, 550, and 750 °C, and the resulting biochar was characterized using diffuse reflectance infrared Fourier transform spectroscopy (DRIFT). Barite-contaminated soils were then treated with biochar and subjected to incubation under flooded conditions for 365 days. Ba concentrations in the soils were analyzed through sequential chemical extraction. The study hypothesized that incorporating biochar produced at high pyrolysis temperatures (750 °C) into soils would elevate soil-solution pH while reducing organic carbon dissolution, thereby buffering redox potential (Eh) and impeding sulfate reduction and Ba dissolution during flooding. The findings offer insights to facilitate the development of sustainable strategies for Ba remediation in flooded environments.

2 Methods

2.1 Soil and barite characterization

A Xanthic Ferralsol (IUSS-WRB 2015) was collected from the topsoil layer (0.2 m) of an area without any record of Ba contamination in Piracicaba, São Paulo State, Brazil (22° 43′ 05″ S 47° 36′ 54″ W). Soil chemical attributes, such as pH $CaCl_2$ (4.4), P (3.3 mg dm^{-3}), K (1.16 $mmol_c$ dm^{-3}), Mg (3.3 $mmol_c$ dm^{-3}), S (12.7 mg dm^{-3}), Fe (26.7 mg dm^{-3}), Mn (7.7 mg dm^{-3}), Al (11.0 $mmol_c$ dm^{-3}), H + Al (64.0 $mmol_c$ dm^{-3}), CEC (79.6 $mmol_c$ dm^{-3}) were determined in triplicate according to Raij et al. (2001). Soil samples were dispersed using 0.1 mol L^{-1} NaOH solution. The sand fraction was sieved and dried (40 °C) whereas silt and clay fractions were separated by siphoning according to Stoke's Law. Granulometric analysis [sand (327 g kg^{-1}), silt (97 g kg^{-1}) and clay (577 g kg^{-1})] was performed in triplicate by the densimeter method (Buoyoucus) according to Gee and Or (2002).

The elemental composition of the soil along with two certified soil samples, a clean sandy loam from Sigma-Aldrich and a San Joaquin soil (2709a) from the National Institute of Standard and Technology were determined in triplicate according to EPA-3051 A protocol (USEPA 2007) (Table A.1). Ba recoveries ranged from 59% (San Joaquin soil; 582 mg kg^{-1}) to 87% (Clean Sandy loam soil; 177 mg kg^{-1}). Total Ba contents of the soil and the barite were evaluated using the EPA-3052 protocol (USEPA 2004), revealing 77,983 mg kg^{-1} of Ba in barite and 7.7 mg kg^{-1} of Ba in the soil. All measurements were performed in triplicate.

2.2 Soil and barite mineralogical analysis

Soil and barite were dried and deposited on a glass sample holder without preferential mineral orientation. X-ray diffraction (XRD) analysis was performed using the XRD tool Rigaku MiniFlex II, with CuKα radiation (0.1540562 nm, 30 kV, and 15 mA). The goniometer speed was 0.02° 2θ s^{-1}, with a sweep ranging from 3 to 60° 2θ. Diffractograms were analyzed in the PANalytical XPert HighScore program. Soil presented a clay mineralogy dominated by kaolinite, hematite, and goethite. Barite's XRD showed peaks corresponding to barite and quartz (data presented in Additional file 1).

2.3 Biochar synthesis and characterization

Sugarcane straw was collected from a freshly harvested area and then pyrolyzed in a sealed double reactor at a

heating rate of 5 °C min^{-1} up to 350, 550, or 750 °C. The residence time at the final temperature was two hours (for more details see Soares et al. 2022a). The elemental composition ($n = 4$) of the three resulting biochars was evaluated by microwave-assisted acid digestion ($HNO_3 + HCl$, 1:10 w/v) according to the International Biochar Initiative (IBI 2015) (Table A.1). The C and N concentrations were determined in an elemental analyzer (LECO, Shimadzu), and ash contents were determined by mass loss in predefined heating ramps using the muffle method (Muffle SP-1200, SPLabor) (ASTM 2007). Specific surface area (SSA) was determined by the Brunauer–Emmett–Teller (BET) method (Song and Guo 2012) utilizing a NOVA-e gas sorption analyzer (Quantachrome). Morphological analyses were performed using scanning electron microscopy (FEI Quanta FEG 250, with a 15 kV beam) (Fig. A.2), and for this, the biochar particles were dispersed on TEM grid using 1 g L^{-1} biochar suspension. Dissolved organic carbon (DOC) was extracted according to Singh et al. (2017) and its concentration was determined using an elementary TOC analyzer (TOC-L, Shimadzu) (Yoon et al. 2018). For this, samples of 5 g of biochar were stirred with 50 mL of deionized water (1:10 w/v) in a horizontal shaker for 1 h at 21 ± 2 °C, and then the samples were filtered through previously calcined 0.45 µm filters.

2.4 Experimental design and treatments

Flooded soils create variable redox conditions that can affect how barite dissolves and moves, potentially releasing Ba and sulfate into the environment. By replicating these conditions over one year, the experiment was designed to mimic real potential risks associated with barite dissolution and its environmental effects. The experiment was conducted in a completely randomized experimental design with four treatments and four replications. The treatments consisted of Ba-contaminated soil without biochar amendment (control) and Ba-contaminated soil amended with sugarcane biochar pyrolyzed at three distinct temperatures: 350 (BC350), 550 (BC550), and 750 °C (BC750).

Each experimental unit consisted of a 150 mL glass flask containing 35 g of soil, 30% carbon (C) in the form of biochar, 1000 mg kg^{-1} of Ba as barite, and 50 mL of ultrapure Milli-Q water (Table A.2). The amount of C was chosen based on the typical C content of wetlands contaminated with Ba in Brazil (Viana et al. 2021a, b). Because each type of biochar differed in its C content, the following masses of biochar were applied to achieve 30% C: BC350 (44.12 g), BC550 (28.46 g), and BC750 (25.73 g). The Ba dose used was higher than the agricultural intervention limit for Ba in Brazil (Table A.2). Soil, biochar, barite, and water were homogenized by shaking in an orbital shaker for 10 min. The experiment was conducted for 365 days at room temperature (25 ± 2 °C), with water added regularly to maintain a 1-cm layer (Fig. A.3). At the end of the experiment, pH and Eh measurements were performed using a portable Hanna pH/ORP meter (model HI 991003). At the end of the experiment, the solution was separated from solids by centrifugation (1845×*g* RCF for 15 min) followed by filtration (0.45 µm cellulose filter).

2.5 Identification of organic functional groups (DRIFT)

Organic functional groups in the solid and solution (dissolved organic carbon, DOC) phases were analyzed using an Alpha II (Bruker$^{\text{ExcludedElement 1T}}$) infrared spectrometer, equipped with a diffuse reflectance (DRIFT) module. Solid-phase samples (< 150 µm) were dried at 45 °C until reaching constant weight and then stored in a desiccator. The solution phase (DOC) was mixed with KBr (1:10 v/w) and then dried at 45 °C until reaching constant weight (Soares et al. 2022a). KBr spectrum (blank) was obtained using DI water. The background spectrum was obtained using a gold-supported sample. The reflectance spectrum (64 scans) was collected from 600 to 4000 cm^{-1} with 2 cm^{-1} resolution. Spectra were preprocessed using the Savitzky–Golay smoothing method, with a 10-point polynomial to reduce electronic and natural oscillations. Atmospheric interference corrections (water vapor and CO_2), background subtraction, and spectral mean were calculated using the OPUS/Mentor software package.

2.6 Ba in solution and its sequential chemical extraction

Dissolved Ba in filtered solution samples (see Sect. 2.4) was quantified by inductively coupled plasma-optical emission spectroscopy (ICP-OES; Thermo Fisher Scientific$^{\text{ExcludedElement 1T}}$, model 1Cap6300 Duo).

To probe Ba forms in the solid phase after incubation, sequential chemical extraction targeting operationally defined pools was adopted combining three methods (Gimeno-García et al. 1995; Siregar et al. 2005; Silveira et al. 2006). For this, aliquots of 2 g of soil (corrected to dry mass) were sequentially extracted four times and generated five fractions: F1 = Ba-exchangeable (Ba-EX, extracted with 1.0 mol L^{-1} $MgCl_2$); F2 = Ba-associated with carbonates and part of Ba-specifically sorbed (Ba-CA, extracted with 1.0 mol L^{-1} sodium acetate adjusted to pH = 5.0); F3 = Ba-more strongly associated with organic matter (Ba-OM, extracted with 6% sodium hypochlorite), F4 = Ba-more strongly associated with Fe and Mn oxides (Ba-OX, extracted with 0.25 mol L^{-1} sodium citrate + 0.11 mol L^{-1} sodium bicarbonate + 3 g sodium dithionite); F5 = Ba-residual (Ba-Res, Ba applied (1000 mg kg^{-1}) minus the sum of previous four fractions). It is important to point out that sodium acetate (pH 5.0) as used in F2 is not limited to carbonate dissolution as

Table 1 Major biochar physicochemical properties as affected by pyrolysis temperatures (350, 550, and 750 °C)

Biochar[1]	C (% w/w)	*N* (% w/w)	C: *N*	DOC (mg L^{-1})	Ash (%)	SSA (m^2 g^{-1})
BC350	34 ± 0.1 b	0.6 ± 0.01 a	57 ± 0.6 c	17.2 ± 0.2 a	5 ± 0.7 c	17 ± 0.8 c
BC550	53 ± 0.4 b	0.7 ± 0.01 b	69 ± 0.9 b	2.0 ± 0.02 b	10 ± 0.2 b	129 ± 13 b
BC750	58 ± 0.02 a	0.6 ± 0.02 a	97 ± 0.3 a	2.0 ± 0.04 b	12 ± 0.3 a	223 ± 14 a

[1] Biochar pyrolyzed at 350, 550, and 750℃; C = total organic carbon; N = total nitrogen; DOC = dissolved organic carbon; and SSA = specific surface area. Means followed by the same letters in the column do not differ (Bootstrap test, $p < 0.05$)

commonly labeled; rather, it can also solubilize metals (Ba) specifically sorbed on clay mineral surfaces, organic matter, and Fe and Mn oxyhydroxides (Ahnstrom and Parker 1999). All extraction solutions were separated from residual solids by centrifugation and filtration, and Ba was quantified by ICP-OES as previously described. As proposed by Kabala and Singh (2001), the Ba mobility factor (MF) was calculated as the ratio of more readily available Ba (F1 + F2) to its total applied amount.

2.7 Statistical analysis

To check the quality of the data and select the most appropriate statistical method for comparing means, all data were subjected to descriptive analysis and the Shapiro-Wilk normality test. The biochar physicochemical data were not normally distributed, so their mean values were compared using a nonparametric Bootstrap test ($p < 0.05$). This test involved comparing mean values using a confidence interval generated by 1,000 random resampling with replacement (Christie 2004). The Bootstrap test was chosen for its practicality, as it does not require data transformation (e.g., normalization by square root or average) or the use of median values. Instead, it allows for working with the actual mean and generates confidence intervals capable of comparing the means of nonparametric data. In the Bootstrap analysis, the calculation power for determining the sample size was based on a power of 90% ($1 - \beta$), a type I error rate (α) of 5%, an anticipated mean difference of 15 ($\mu A - \mu B$), an estimated standard deviation of 5, and a sampling ratio of 1 (equal-sized groups). Based on these estimates, the required sample size was determined to be 4.

Soil data were contrasted using the Tukey test ($p < 0.05$). All statistical calculations were performed using the R program (R Core Team, Vienna, Austria).

3 Results and discussion

3.1 Major biochar physicochemical attributes

The ash, carbon (C) contents, and specific surface area (SSA) of biochar increased with pyrolysis temperatures (Table 1). The specific surface area (SSA) of BC550 and BC750 was 7.6 times and 13.1 times greater than that of BC350. However, BC350 had over 8 times more dissolved organic carbon (DOC) than BC550 and BC750, indicating lesser stability. Because SSA influences adsorptive capacity and DOC correlates with reducing capacity, BC350 may be more effective at promoting barite reduction with less ability to adsorb dissolved Ba, whereas BC550 and BC750 should have greater adsorptive capacities with lesser reducing capacity.

3.2 Diffuse reflectance spectra (DRIFT)

Amending soil with high-temperature biochar (> 550 °C) decreased C–O signals associated with polysaccharide (1110–1042 cm^{-1}) and carboxylic (~ 1730 cm^{-1}) groups (as compared to the unamended control) in the aqueous phase (DOC, Fig. 1a). Biochar contains functional groups capable of sorbing DOC through hydrophobic bonds or π–π electron–donor–acceptor (EDA) interactions (Sun et al. 2012; Zhu and Pignatello 2005), which could reduce vibrations among oxygenated functional groups, as seen in our results (Fig. 1a). High-temperature biochar (BC550 and BC750) has a large SSA (Table 1), indicating the potential for sorbing DOC. It is also important to note that higher pyrolysis temperatures alter C-structure, increase dehydration and depolymerization (Zhang et al. 2017), and release volatile substances and carbonaceous gases (Fig. 1a, Table A.4), resulting in more stable biochar that tends to release less DOC, aligning with our previous results (Table 1).

For the solid phase, biochar addition increased the peak signals for COOH (1730 cm^{-1}), C=O (1512 cm^{-1}), and phenolic-OH (1400 cm^{-1}) with decreasing the intensity of C–O groups associated with polysaccharides (1110–1042 cm^{-1}) (Fig. 1b; Table A.4). The major spectral differences were in the < 1800 cm^{-1} region, where biochar increased signals associated with aromatic (C–H) and lignocellulose (C=O) groups but reduced the (C–O) signal associated with polysaccharides. A similar result was observed for bulk biochar samples alone (Soares et al. 2022b).

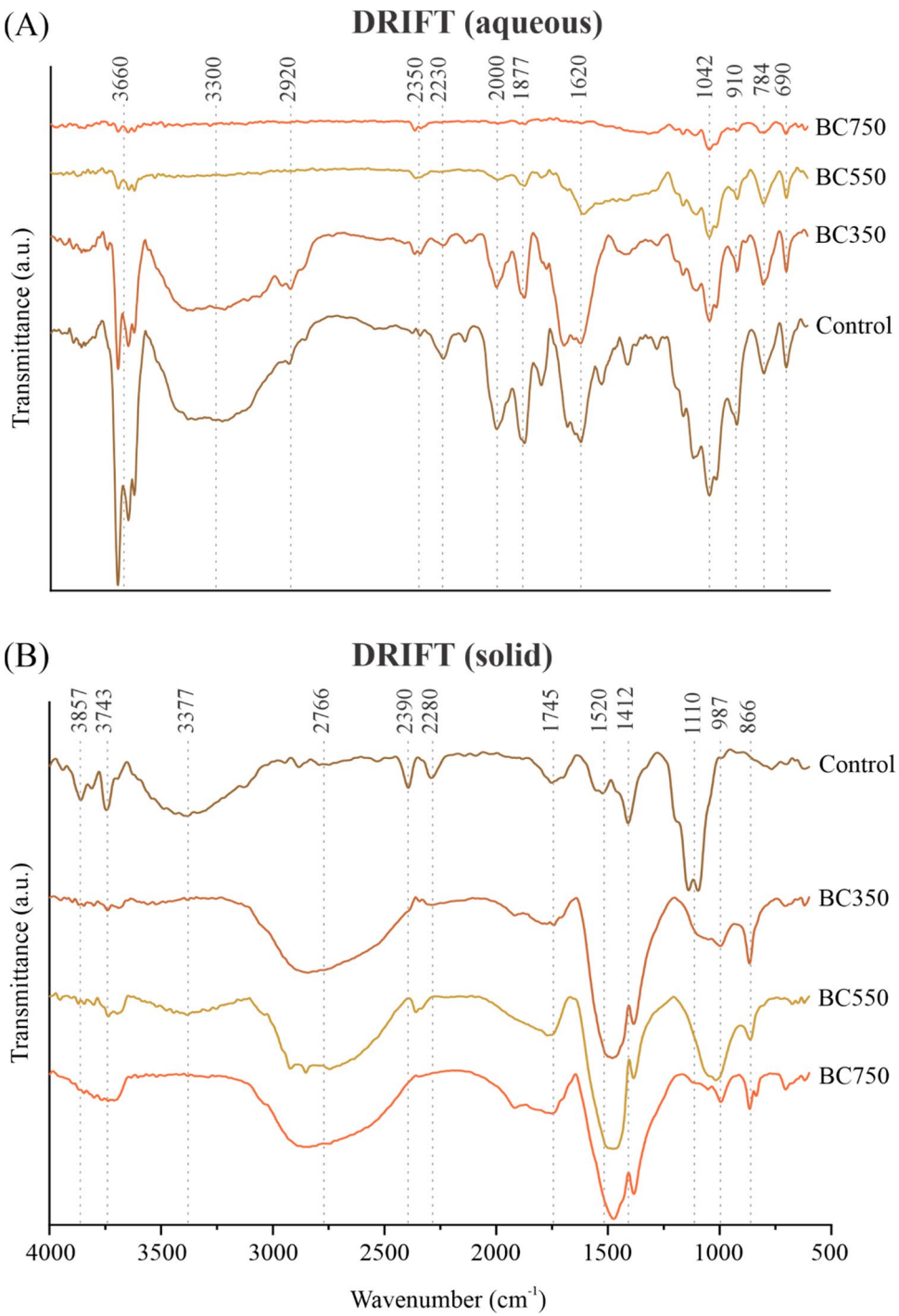

Fig. 1 Diffuse reflectance infrared Fourier transform (DRIFT) spectra for the soil (control) and the soil amended with biochar pyrolyzed at 350, 550, and 750 °C in the liquid (aqueous) (**a**) and solid (**b**) phases. Details are presented in Additional file 1: Table A1)

3.3 pH and redox potential (Eh)

Soil pH increased monotonically with the pyrolysis temperature of the biochar amendment (pH = 5.9, 7.5, 8.6, and 9.2 for control, BC350, BC550, and BC750, respectively) (Fig. 2a). Biochar synthesis produces alkaline substances in the ash, such as calcium carbonate and phosphate minerals, which can raise soil solution pH (Novak et al. 2009; Yuan et al. 2011). Our results (Table 1) are consistent with Tan et al. (2020), who showed that higher pyrolysis temperatures result in biochar with

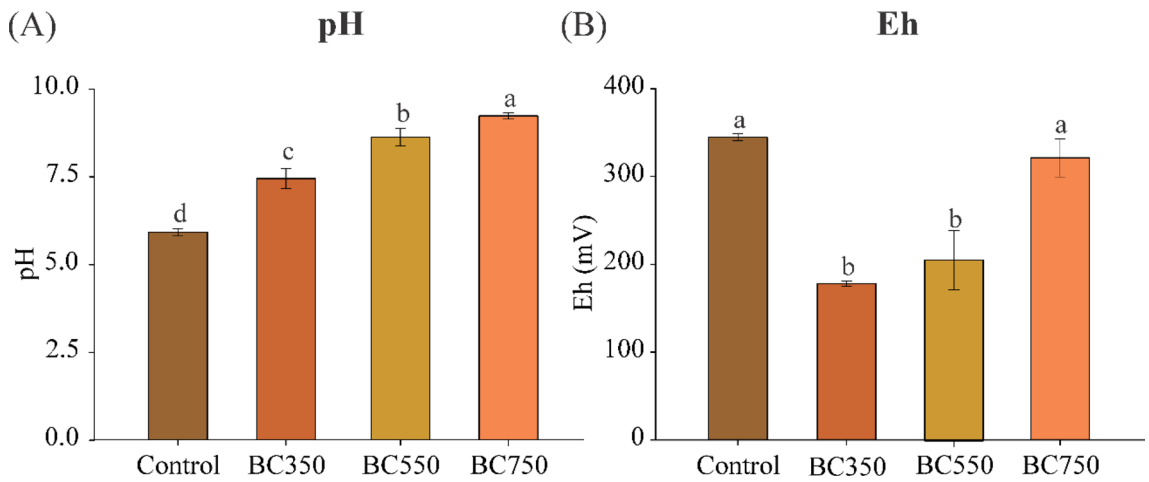

Fig. 2 Soil-pH (**a**) and redox potential (Eh, **b**) in the soil (control) and the soil amended with biochar pyrolyzed at 350, 550, and 750 °C. Means followed by the same letters do not differ (Tukey test, $p < 0.05$)

higher ash content, containing metal alkali oxides that increase biochar alkalinity. The higher pH may also result from the loss of organic acid functional groups (e.g., –OH and –COOH) through dehydration and depolymerization during pyrolysis (Zhang et al. 2017), supported by the decrease in vibration signals of OH and –C=O groups (Fig. 1a; Table A.4).

Solution pH is a major factor influencing biochar capacity for binding cationic metals (Younis et al. 2020; Shin et al. 2021). For example, spent coffee biochar showed greater Ba removal from contaminated water when pre-exposed to solutions with a pH > 7, which affects surface binding moieties (Shin et al. 2021). The adsorptive removal of Ba^{2+} was significantly influenced by electrostatic attractive interactions with the biochar surfaces due to a decrease in surface zeta potential with increasing pH, indicating a more negatively charged surface. Here, the decrease in oxygenated functional groups (Fig. 1) resulted in more alkaline conditions (Fig. 2), especially at higher pyrolysis temperatures, leading to an increase in negatively charged biochar surfaces, electrostatically favoring sorption.

Compared to the control (Eh = 345 mV), soil Eh decreased by 48% (179 mV), 40% (207 mV), and 7% (321 mV) when amended with BC350, BC550, and BC750, respectively (Fig. 2b). High-temperature biochar (BC750) is often associated with the transformation of labile-C into more stable forms (C-aromatic) and lesser DOC contents (Table 1), which may explain its lessened contribution to electron transfer reactions (Zhang et al. 2017; Yuan et al. 2019), limiting its impact on Eh. The biochar BC350 was applied at greater rates than BC550 (1.56×) and BC750 (1.70×). This increased loading and the greater DOC contents of low temperature biochar

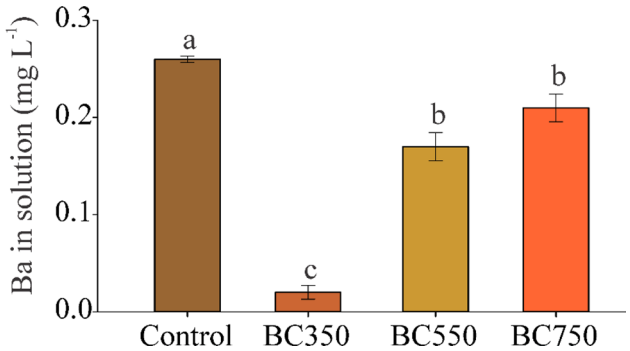

Fig. 3 Ba concentrations in the aqueous phase (solution). Control = soil and BC350, BC550, and BC750 = soil amended with biochar pyrolyzed 350, 550, and 750 °C, respectively. Means followed by some letters do not differ (Tukey test, $p < 0.05$)

suggest that a calculated 13.4 and 14.6 times more DOC was added with BC350 compared to BC550 and BC750, respectively, whereas the DOC addition for BC550 was only 1.09× greater than for BC750.

DOC typically consists of low molecular weight molecules with lower aromaticity that are susceptible to abiotic and biotic degradation, which may occur under reducing conditions (Liu et al. 2019). Soares et al. (2023) used deconvolution of FTIR spectra to characterize DOC from BC350 and BC750, observing that compounds with low thermal stability, mainly polysaccharides, were lost (converted to CO_2) with heating. Low thermal stability compounds decreased from 38% (BC350) to 4.7% (BC750), whereas highly stable compounds, such as those containing aromatic groups, increased from 15.9% (BC350) to 64.5% (BC750). The presence of sugars and polysaccharides in the DOC fraction may have favored

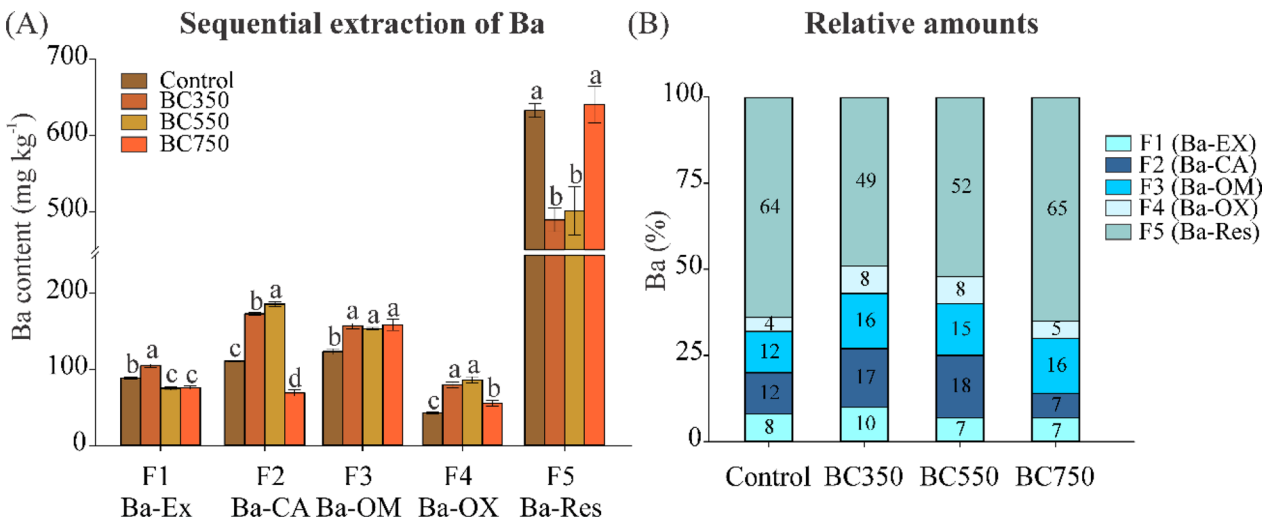

Fig. 4 Sequential extraction of Ba (**a**) and its relative amounts (**b**). Control = soil and BC350, BC550, and BC750 = soil amended with biochar pyrolyzed 350, 550, and 750 °C, respectively. F1 (Ba-EX) = exchangeable Ba; F2 (Ba-CA) = Ba associated with carbonates and part of Ba sorbed specifically, F3 (Ba-OM) = Ba more strongly associated with organic matter, F4 (Ba-OX) = Ba more strongly associated with oxides; and F5 (Ba-Res) = Ba residual. Means followed by the same letter did not differ within each fraction (Tukey test, $p < 0.05$)

microbial activity, primarily in BC350 but also in BC550, leading to Eh reduction in both. The lack of these compounds at pyrolysis temperatures > 700 °C (Tomczyk et al. 2020; Yi et al. 2022) may have inhibited microbial growth and soil reduction in BC750. The rate of organic matter oxidation can decrease due to the relative accumulation of residual aromatic and aliphatic compounds (Gunina and Kuzyakov 2022). Consequently, not only the lower DOC for BC750 (Table 1) but also the increase in aliphatic domains (Fig. 1) may have resulted in a less reducing the soil geochemical environment (Eh > 300 mV) even under saturated conditions (Fig. 2), and thus decreased barite reductive dissolution.

An alternative for increasing the potential of high-temperature sugarcane straw biochar for barite dissolution and Ba remediation could be biochar modification, where oxygen-containing functional groups are produced on the biochar surface through chemical activation (e.g., alkalization) (Shin et al. 2021). For instance, oxidation and thiolation treatments enhanced the polarity, surface area, and pore volume of pig manure biochar produced at 700 °C (Wang et al. 2021).

3.4 Ba in the aqueous phase (solution)

Biochar addition to soils decreased Ba concentrations in solution, with the dissolved Ba concentrations increasing monotonically with increasing pyrolysis temperatures (0.02, 0.17, and 0.21 mg L^{-1} for BC350, BC550, and BC750, respectively) (Fig. 3). In all cases, the Ba mass in solution corresponded to less than 0.05% of its applied amount but reached up to 30% of the Brazilian freshwater standard (0.70 mg L^{-1}, CONAMA 2009).

Rice straw biochar produced at 550 °C adsorbed 73.9 mg of Ba per gram of biochar from saline solutions, removing 97.5% of the total Ba concentration (Younis et al. 2020). This removal rate is comparable to our work, especially for BC350, which removed 92% of the Ba from the solution as to the control (Fig. 3).

3.5 Ba geochemical fractionation (sequential extraction)

In soils, Ba was primarily associated with the residual fraction (F5), which accounted for at least 49% of its applied amount (Fig. 4a, b). F5 was greatest for BC750 and the control (~ 65%), followed by BC550 (52%) and BC350 (49%) (Fig. 4b). Assuming that F5 is composed of barite, compared to the control, 23.4% and 18.8% of the barite was dissolved from BC350 and BC550, respectively, whereas no addition barite was dissolved from BC750. This trend suggests that Ba present in barite is more readily dissolved under the more reducing conditions associated with low temperature biochar amendment (Fig. 2b). Although the measured Eh values for BC350 and BC550 were above the published potential for sulfate reduction (−100 mV, Otero et al. 2009), bulk measurements do not preclude this reaction at more reducing microsites present in the soil. The control and BC750 remained under oxic conditions, thus limiting Ba solubilization. Indeed, Ba in the more labile fractions (F1 and F2) of the soil was higher for BC350 (10% and 8%, respectively) and lower for BC750 (7% and 5%, respectively) (Fig. 4b), despite

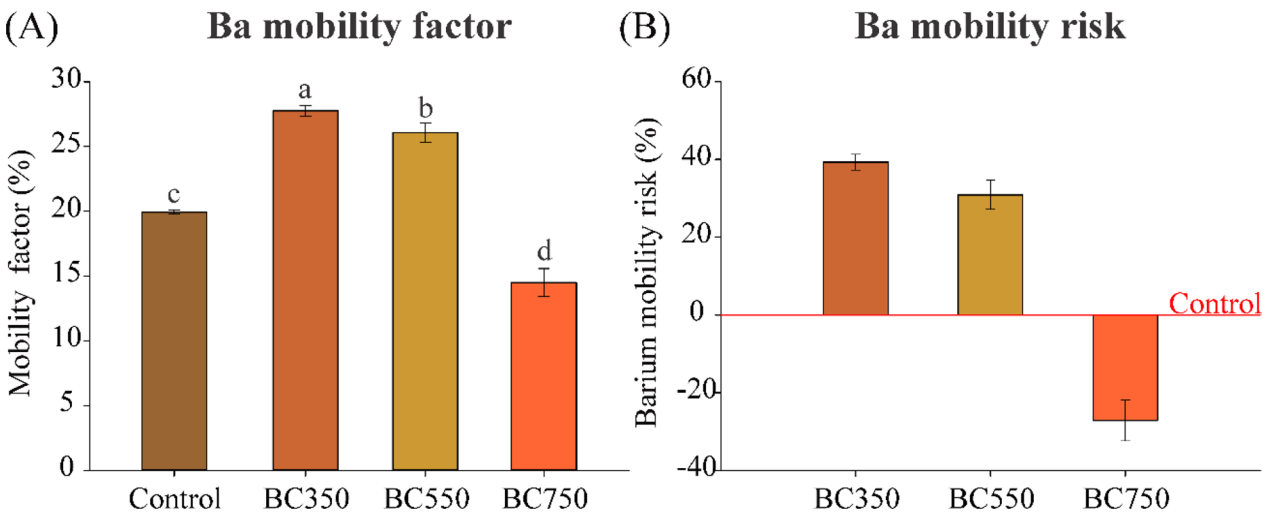

Fig. 5 Calculated Ba mobility factor (**a**) and its relative values (**b**) in the soil (control) and the soil amended with biochar pyrolyzed at 350, 550, and 750 °C. Means followed by the same letter did not differ (Tukey test, $p < 0.05$)

BC750 presenting higher Ba contents in solution (Fig. 3). Taken in total, our results indicate that low-temperature biochar tends to have higher labile organic-C contents, which can favor carbon utilization by microbes and create reducing conditions (Hamer et al. 2004; Awad et al. 2012), enhancing barite dissolution. BC350, for example, had more reducing conditions (lower Eh; Fig. 2), which likely favored barite reductive dissolution and Ba release. This released Ba could either remain in solution or be retained (sorbed) into distinct soil fractions. Low-temperature biochar, such as BC350, tends to have higher cation exchange capability (CEC) due to its higher contents of oxygen-containing functional groups like –COH and –COOH (Melo et al. 2013), which may favor Ba sorption through non-specific or specific mechanisms, such as electrostatic interactions and Ba complexation (C=O–Ba complex), respectively. Specific interactions are likely less concerning for Ba than for other PTEs because Ba has one of the largest ionic radii among the 2 A-elements group and has a high coordination number with carboxylic ligands (Yun et al. 2016).

Conversely, high-temperature biochar, such as BC750, tends to contain more recalcitrant aromatic groups (Fig. 1) and lower DOC content (Table 1) and thus may not promote the formation of reducing conditions (Fig. 2; Qiu et al. 2020). This characteristic makes high-temperature biochar less likely to promote reductive barite dissolution. At greater temperatures (≥600 °C), biochar aromatization enhances the formation of π bonds capable of forming hydrogen bonds with water (Tan et al. 2020), thereby reducing the number of available sites for exchangeable cation sorption (van Poucke et al. 2019). High-temperature biochar also has fewer deprotonated oxygen-containing functional groups and a lower point of zero charge, contributing to its reduced capacity to sorb cations (Tan et al. 2020). This lesser sorption capacity may help to explain why high-temperature biochar has a greater dissolved Ba concentration despite the greater fraction of unreduced barite remaining in the residual fraction.

Shifts in biochar speciation in both the aqueous and solid phases affected barite dissolution and Ba mobility in the soils. Despite suggested greater sorption, BC350 showed a higher Ba mobility factor (Fig. 5a) and greater Ba mobility risk (Fig. 5b), likely due to increased barite dissolution (Fig. 2). BC550 displayed intermediate behavior, whereas BC750 had the lowest Ba mobility factor and reduced Ba mobility risk by 27% compared to the control (Fig. 5b). The higher pH of BC550 (8.6) and especially BC750 (9.2) may promote co-precipitation of released Ba and specific adsorption onto residual soil iron oxides (Ouyang et al. 2019).

Our results showed that different pyrolysis temperatures impacted the biochar adsorptive capacity, ultimately affecting Ba mobility and the mobility risk (Fig. 5). Those results are similar to other experiments with different pollutants (Alexandre et al. 2023; Soares et al. 2024). Sugarcane biochar pyrolyzed at 750 °C reduced Pb leaching by 54% whereas the biochar pyrolyzed at 350 °C increased As mobility 2.5 times (Soares et al. 2024). As an additional benefit for its use in remediation, sugarcane biochar also has the potential to decrease the ecotoxicity of pesticides in soils (Alexandre et al. 2023), reducing Fipronil and 2,4-D harmful effects on eudicot plant *Eruca sativa* L. and also the terrestrial worm *Enchytraeus crypticus*.

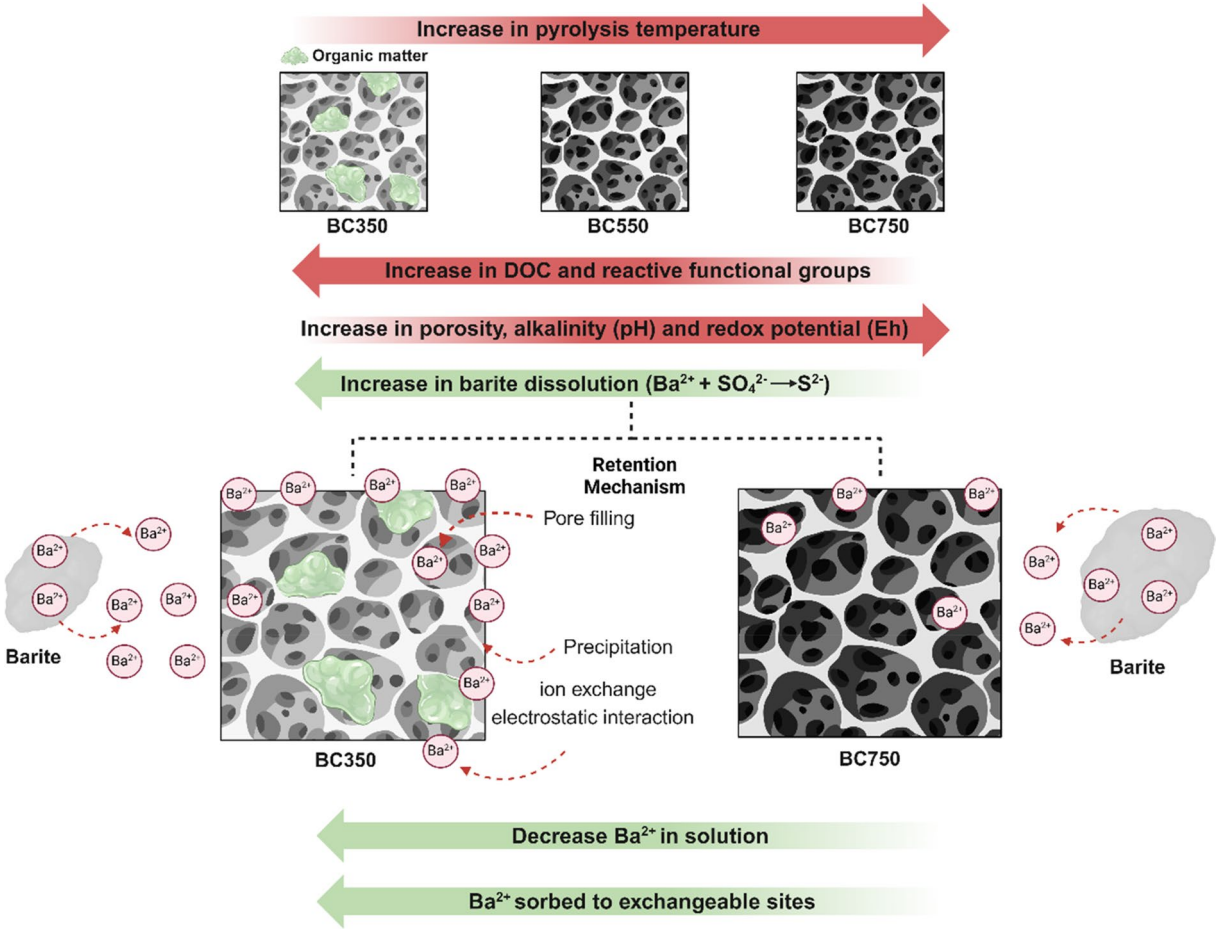

Fig. 6 Conceptual model of biochar characteristics impact on barite dissolution and barium mobility in soils

4 Environmental implications and concluding remarks

The efficacy of sugarcane straw biochar for Ba remediation was affected by biochar pyrolysis temperature because it directly affects biochar attributes, such as carbon and ash contents, oxygenated functional group density, and dissolved organic carbon release. In turn, these properties will affect soil pH and redox potential, thus altering barite dissolution and sorption of dissolved Ba on solids (Fig. 6). Understanding how these biochar properties affect Ba speciation and mobility is essential for developing effective remediation strategies that minimize secondary environmental impacts, such as the release of other contaminants or changes in soil chemistry. This knowledge can help optimize biochar production methods to maximize remediation efficiency while ensuring environmental safety.

Higher pyrolysis temperatures, especially at 750 °C, generally increase the SSA and porosity and can promote the formation of more stable carbon structures and functional groups that are often more effective in binding heavy metals. Its amendment increases environmental pH without a large decrease in redox potential (Fig. 6). This condition inhibits sulfate reduction and barite dissolution. However, biochar modifications at high temperatures limit Ba sorption, particularly into more labile soil fractions like exchangeable sites, decreasing the available pool in the soil but increasing dissolved concentrations. Conversely, low pyrolysis temperature biochar, especially at 350 °C, had higher DOC content, and more reduced soil conditions (lower Eh), leading to a 23.4% enhancement in barite reductive dissolution and an increase in the available pool of Ba in the soil, despite its lower dissolved content in solution (Fig. 6). Therefore, low-temperature biochar may be used to enhance Ba availability in assisted remediation programs, such as biochar-assisted phytoremediation (Shaheen et al. 2023).

Previous research on using biochar for Ba remediation has mainly focused on water treatment (Younis et al. 2020; Shin et al. 2021; Zuhara and McKay 2024). To the authors' knowledge, biochar application for Ba

remediation in flooded soils is an unexplored technique. In this initial attempt, we used barite-spiked soils in a batch experiment simulating wetlands. Although this study provides valuable insights into the potential of sugarcane straw biochar for Ba remediation in flooded soils, there are several avenues for further investigation, including trials at Ba-contaminated sites. Future research could delve into the long-term effectiveness and stability of biochar-mediated Ba remediation under varying environmental conditions. Moreover, assessing the potential impact of biochar application on soil microbial communities would be beneficial. Finally, exploring the economic feasibility and scalability of biochar application for large-scale remediation projects is crucial for its practical implementation in contaminated sites.

Supplementary Information

The online version contains supplementary material available at https://doi.org/10.1007/s42773-024-00371-w.

Additional file 1.

Acknowledgements
The authors gratefully thank Fundação de Estudos Agrários Luiz de Queiroz (FEALQ), the São Paulo Research Foundation (FAPESP) (Grant Nos. 2019/02796-3; 2019/22280-1) and the Coordenação de Aperfeiçoamento de Pessoal de Nível Superior—Brasil (CAPES), Finance Code 001 for the scholarship for this research. M.B.S gratefully thanks the FAPESP (Grant Nos. 2019/06897-9; 2020/13700-4) and the Brazilian Council for Scientific and Technological Development—Conselho Nacional de Desenvolvimento Científico e Tecnológico (CNPq) for the scholarships (Grant Nos. 140830/2018-9 and 311514/2023-5). O.W.D was supported by the USDA National Institute of Food and Agriculture, Hatch projects NC02713 and NC02951.

Author contributions
The manuscript was written through the contributions of all authors. All authors read and approved the final manuscript.

Funding
São Paulo Research Foundation (FAPESP); Coordenação de Aperfeiçoamento de Pessoal de Nível Superior—Brasil (CAPES), Conselho Nacional de Desenvolvimento Científico e Tecnológico (CNPq) and USDA.

Availability of data and materials
The datasets generated and/or analyzed during the current study are not publicly available due [REASON WHY DATA ARE NOT PUBLIC] but are available from the corresponding author on reasonable request.

Declarations

Ethics approval and consent to participate
Not applicable.

Consent for publication
Not applicable.

Competing interests
The authors declare that they have no competing interests.

Author details
[1]Department of Soil Science, Luiz de Queiroz College of Agriculture (ESALQ), University of São Paulo (USP), Piracicaba, SP, Brazil. [2]Department of Crop and Soil Sciences, North Carolina State University, Raleigh, NC, USA. [3]Department of Chemistry, Institute of Exact Sciences, Federal University of Minas Gerais, Belo Horizonte, MG, Brazil.

Received: 29 January 2024 Revised: 10 July 2024 Accepted: 30 July 2024
Published online: 08 October 2024

References

Ahnstrom ZS, Parker DR (1999) Development and assessment of a sequential extraction procedure for the fractionation of soil cadmium. Soil Sci Soc Am J 63(6):1650–1658. https://doi.org/10.2136/sssaj1999.6361650x

Ambaye TG, Vaccari M, van Hullebusch ED, Amrane A, Rtimi S (2021) Mechanisms and adsorption capacities of biochar for the removal of organic and inorganic pollutants from industrial wastewater. Int J Environ Sci Technol 18:3273–3294. https://doi.org/10.1007/s13762-020-03060-w

ASTM (2007) Standard test method for chemical analysis of wood charcoal. https://www.astm.org/d1762-84r21.html. Accessed March 1, 2022

Awad YM, Blagodatskaya E, Ok YS, Kuzyakov Y (2012) Effects of polyacrylamide, biopolymer, and biochar on decomposition of soil organic matter and plant residues as determined by 14 C and enzyme activities. Eur J Soil Biol 48:1–10. https://doi.org/10.1016/j.ejsobi.2011.09.005

Bouslimi H, Ferreira R, Dridi N, Brito P, Martins-Dias S, Cacador I, Sleimi N (2021) Effects of barium stress in *Brassica juncea* and *Cakile maritima*: the indicator role of some antioxidant enzymes and secondary metabolites. Phyton. https://doi.org/10.32604/phyton.2020.011752

Carvalho CFMD, Viana DG, Pires FR, Egreja Filho FB, Bonomo R, Martins LF, Cruz LBS, Nascimento MCP, Cargnelutti Filho A (2019) Phytoremediation of barium-affected flooded soils using single and intercropping cultivation of aquatic macrophytes. Chemosphere. https://doi.org/10.1016/j.chemosphere.2018.09.096

Chałupnik S, Wysocka M, Chmielewska I, Samolej K (2019) Radium removal from mine waters with the application of barium chloride and zeolite: comparison of efficiency. J Sustain Mining 18(4):174-181. https://doi.org/10.1016/j.jsm.2019.07.002

Chen G, Zhang Z, Zhang Z, Zhang R (2018) Redox-active reactions in denitrification provided by biochars pyrolyzed at different temperatures. Sci Total Environ 615:1547–1556. https://doi.org/10.1016/j.scitotenv.2017.09.125

Chen M, Wang D, Xu X, Zhang Y, Gui X, Song B, Xu N (2022) Biochar nanoparticles with different pyrolysis temperatures mediate cadmium transport in water-saturated soils: effects of ionic strength and humic acid. Sci Total Environ 806:150668. https://doi.org/10.1016/J.SCITOTENV.2021.150668

Cherubin MR, Lisboa IP, Silva AGB, Varanda LL, Bordonal RO, Carvalaho JLN, Otto R, Pavinato PS, Soltangheisi A, Cerri CEP (2019) Sugarcane straw removal: implications to soil fertility and fertilizer demand in Brazil. Bioenerg.Res.12:888–900. https://doi.org/10.1007/s12155-019-10021-w

Choudhury H, Cary R (2001) Concise international chemical assessment document. Barium and barium compounds, pp 5–10

Christie D (2004) Resampling with Excel. Teach Stat 26:9–14. https://doi.org/10.1111/J.1467-9639.2004.00136.X

CONAMA, (Environment National Council) (2009) Resolution No. 420 of December 28, 2009 (in Portuguese). Accessed 23 Jan 2022

Dallas CE, Williams PL (2011) Barium: Rationale for a new oral reference dose. J Toxicol Environ Health B Crit Rev 4:395–429. https://doi.org/10.1080/109374001753146216

de Souza Cardoso AA, Monteiro FA (2021) Sulfur supply reduces barium toxicity in Tanzania Guinea grass (Panicum maximum) by inducing antioxidant enzymes and proline metabolism. Ecotoxicol Environ Saf 208:111643. https://doi.org/10.1016/j.ecoenv.2020.111643

El-Naggar A, Shaheen SM, Ok YS, Rinklebe J (2018) Biochar affects the dissolved and colloidal concentrations of Cd, Cu, Ni, and Zn and their phytoavailability and potential mobility in a mining soil under dynamic redox-conditions. Sci Total Environ 624:1059–1071. https://doi.org/10.1016/j.scitotenv.2017.12.190

Ghaemi A, Torab-Mostaedi M, Ghannadi-Maragheh M (2011) Characterizations of strontium (II) and barium (II) adsorption from aqueous solutions using dolomite powder. J Hazard Mater 190(1–3):916–921

Gimeno-García E, Andreu V, Boluda R (1995) Distribution of heavy metals in rice farming soils. Arch Environ Contam Toxicol 29(4):476–483. https://doi.org/10.1007/BF00208377

Gunina A, Kuzyakov Y (2022) From energy to (soil organic) matter. Glob Change Biol 28(7):2169–2182. https://doi.org/10.1111/gcb.16071

Hamer U, Marschner B, Brodowski S, Amelung W (2004) Interactive priming of black carbon and glucose mineralisation. Org Geochem 35(7):823–830. https://doi.org/10.1016/J.ORGGEOCHEM.2004.03.003

IBI (2015) Standardized product definition and product testing guidelines for biochar that is used in soil

IUSS Working Group WRB (2015) World Reference Base for Soil Resources 2014, update 2015 International soil classification system for naming soils and creating legends for soil maps. FAO, Rome

Kabala C, Singh BR (2001) Fractionation and mobility of copper, lead, and zinc in soil profiles in the vicinity of a copper smelter. J Environ Qual 30:485–492. https://doi.org/10.2134/JEQ2001.302485X

Kampf N, Schwertmann U (1982) The 5-M-NaOH concentration treatment for iron oxides in soils. Undefined 30:401–408. https://doi.org/10.1346/CCMN.1982.0300601

Li J, Dai J, Liu G, Zhang H, Gao Z, Fu J, He Y, Huang Y (2016) Biochar from microwave pyrolysis of biomass: a review. Biomass Bioenergy 94:228–244. https://doi.org/10.1016/j.biombioe.2016.09.010

Ma L, Hu T, Liu Y, Liu J, Wang Y, Wang P, Zhou J, Chen M, Yang B, Li L (2021) Combination of biochar and immobilized bacteria accelerates polyacrylamide biodegradation in soil by both bio-augmentation and bio-stimulation strategies. J Hazard Mater 405:124086. https://doi.org/10.1016/J.JHAZMAT.2020.124086

Manya JJ (2012) Pyrolysis for Biochar purposes: a review to establish current knowledge gaps and Research needs. Environ Sci Technol 46:7939–7954. https://doi.org/10.1021/es301029g

Martíni AF, Valani GP, Boschi RS, Bovi RC, Simões da Silva LF, Cooper M (2020) Is soil quality a concern in sugarcane cultivation? A bibliometric review. Soil Tillage Res 204:104751. https://doi.org/10.1016/J.STILL.2020.104751

Melo LC, Coscione AR, Abreu CA, Puga AP, Camargo OA (2013) Influence of Pyrolysis Temperature on Cadmium and Zinc Sorption Capacity of Sugar Cane Straw--Derived Biochar. BioResources 8(4)

Mukherjee S, Thakur AK, Goswami R, Mazumder P, Taki K, Vithanage M, Kumar M (2021) Efficacy of agricultural waste derived biochar for arsenic removal: tackling water quality in the Indo-Gangetic plain. J Environ Manage 281:111814. https://doi.org/10.1016/J.JENVMAN.2020.111814

Novak JM, Lima I, Xing B, Gaskin JW, Steiner C, Das KC, Ahmedna M, Rehrah D, Watts DW, Busscher WJ, Schomberg H (2009) Characterization of designer Biochar Produced at different temperatures and their effects on a Loamy Sand. Annals Environ Sci 3:195–206

Ouyang B, Renock DJ, Ajemigbitse MA, Van Sice K, Warner NR, Landis JD, Feng X (2019) Radium in hydraulic fracturing wastewater: distribution in suspended solids and implications to its treatment by sulfate co-precipitation. Environ Science: Processes Impacts 21(2):339–351. https://doi.org/10.1039/C8EM00311D

Qian W, Liang JY, Zhang WX, Huang ST, Diao ZH (2022) A porous biochar supported nanoscale zero-valent iron material highly efficient for the simultaneous remediation of cadmium and lead contaminated soil. J Environ Sci 113:231–241. https://doi.org/10.1016/J.JES.2021.06.014

Qiu YY, Zhang L, Mu X, Li G, Guan X, Hong J, Jiang F (2020) Overlooked pathways of denitrification in a sulfur-based denitrification system with organic supplementation. Water Res 169:115084. https://doi.org/10.1016/j.watres.2019.115084

Raij BV, Andrade JC, Cantarella H, Quaggio JA (2001) Análise química para avaliação da fertilidade de solos tropicais (in Portuguese). Instituto Agronômico, Campinas, Campinas

Rinklebe J, Shaheen SM, El-Naggar A, Wang H, Du Laing G, Alessi DS, Ok YS (2020) Redox-induced mobilization of Ag, Sb, Sn, and Tl in the dissolved, colloidal and solid phase of a biochar-treated and un-treated mining soil. Environ Int 140:105754. https://doi.org/10.1016/j.envint.2020.105754

Shen Z, Zhang Z, Zhang M, Rinklebe J, Ma Y, Hou D (2021) Effect of production temperature and particle size of rice husk biochar on mercury immobilization and erosion prevention of a mercury contaminated soil. J Hazard Mater 420:126646. https://doi.org/10.1016/J.JHAZMAT.2021.126646

Shin J, Kwak J, Lee Y-G, Kim S, Son C, Cho KH, Lee S-H, Park Y (2021) Xianghao Ren, and Kangmin Chon. Changes in adsorption mechanisms of radioactive barium, cobalt, and strontium ions using spent coffee waste biochars via alkaline chemical activation: Enrichment effects of O-containing functional groups. Environ Res 199:111346

Siregar A, Kleber M, Mikutta R, Jahn R (2005) Sodium hypochlorite oxidation reduces soil organic matter concentrations without affecting inorganic soil constituents. Eur J Soil Sci 56:481–490. https://doi.org/10.1111/J.1365-2389.2004.00680.X

Soares MB, Cerri CEP, Demattê JAM, Alleoni LRF (2022a) Biochar aging: impact of pyrolysis temperature on sediment carbon pools and the availability of arsenic and lead. Sci Total Environ 807:151001. https://doi.org/10.1016/J.SCITOTENV.2021.151001

Soares MB, Duckworth OW, Alleoni LR (2023) The role of dissolved pyrogenic carbon from biochar in the sorption of as (V) in biogenic iron (oxyhydr) oxides. Sci Total Environ 865:161286. https://doi.org/10.1016/j.scitotenv.2022.161286

Soares MB, Ferreira JR, Colzato M et al (2024) Role of pyrolysis temperature on arsenic and lead leaching potential in a biochar-amended sediment. Int J Environ Res 18:51. https://doi.org/10.1007/s41742-024-00604-7

Solano-Rodríguez B, Pye S, Li P-H, Ekins P, Manzano O, Vogt-Schilb A (2021) Implications of climate targets on oil production and fiscal revenues in Latin America and the Caribbean. Energy Clim Change 2:100037. https://doi.org/10.1016/J.EGYCC.2021.100037

Song W, Guo M (2012) Quality variations of poultry litter biochar generated at different pyrolysis temperatures. J Anal Appl Pyrol 94:138–145. https://doi.org/10.1016/J.JAAP.2011.11.018

Sun K, Jin J, Keiluweit M, Kleber M, Wang Z, Pan Z, Xing B (2012) Polar and aliphatic domains regulate sorption of phthalic acid esters (PAEs) to biochars. Bioresour Technol 118:120–127. https://doi.org/10.1016/j.biortech.2012.05.008

Tan Z, Yuan S, Hong M, Zhang L, Huang Q (2020) Mechanism of negative surface charge formation on biochar and its effect on the fixation of soil cd. J Hazard Mater 384:121370. https://doi.org/10.1016/J.JHAZMAT.2019.121370

Tang J, Johannesson KH (2010) Ligand extraction of rare earth elements from aquifer sediments: implications for rare earth element complexation with organic matter in natural waters. Geochim Cosmochim Acta 74(23):6690–6705. https://doi.org/10.1016/j.gca.2010.08.028

Tao H, Man Y, Shi X, Zhu J, Pan H, Qin Q, Liu S (2016) Inconceivable hypokalemia: a case report of acute severe barium chloride poisoning. Case reports in medicine. 2016(1):2743134. https://doi.org/10.1155/2016/2743134

Tomczyk A, Sokołowska Z, Boguta P (2020) Biochar physicochemical properties: pyrolysis temperature and feedstock kind effects. ReviewsEnviron Sci Bio/Technol 19:191–215. https://doi.org/10.1007/s11157-020-09523-3

USEPA (2002) National primary drinking water regulations. Office of Ground Water and Drinking Water. http://www.epa.gov/safewater/consumer/pdf/mcl.pdf

USEPA (2004) Method 3052 Microwave Assisted Acid Digestion of Siliceous and Organically Based Matrices, EPA SW-846, Revision 3. Washington DC

USEPA (2005) Ecological soil screening levels for barium. https://rais.ornl.gov/documents/eco-ssl_barium.pdf

USEPA (2007) Method 3051A: Microwave-assisted acid digestion of sediments, sludges, soils and oils. EPA, Washington

van Poucke R, Allaert S, Ok YS, Pala M, Ronsse F, Tack FMG, Meers E (2019) Metal sorption by biochars: a trade-off between phosphate and carbonate concentration as governed by pyrolysis conditions. J Environ Manage 246:496–504. https://doi.org/10.1016/J.JENVMAN.2019.05.112

Viana DG, Egreja Filho FB, Pires FR, Soares MB, Ferreira AD, Bonomo R, Martins LF (2021a) In situ barium phytoremediation in flooded soil using Typha domingensis under different planting densities. Ecotoxicol Environ Saf 210:111890. https://doi.org/10.1016/J.ECOENV.2021.111890

Viana DG, Pires FR, Ferreira AD, Egreja Filho FB, de Carvalho CFM, Bonomo R, Martins LF (2021b) Effect of planting density of the macrophyte consortium of Typha domingensis and Eleocharis acutangula on phytoremediation of barium from a flooded contaminated soil. Chemosphere 262:127869. https://doi.org/10.1016/J.CHEMOSPHERE.2020.127869

Vithanage M, Mayakaduwa SS, Herath I, Ok YS, Mohan D (2016) Kinetics, thermodynamics and mechanistic studies of carbofuran removal using biochars from tea waste and rice husks. Chemosphere 150:781–789. https://doi.org/10.1016/j.chemosphere.2015.11.002

Wang J, Wang S (2019) Preparation, modification and environmental application of biochar: a review. J Clean Prod 227:1002–1022. https://doi.org/10.1016/J.JCLEPRO.2019.04.282

Wang SP, Wang L, Sun ZY, Wang ST, Shen CH, Tang YQ, Kida K (2021) Biochar addition reduces nitrogen loss and accelerates composting process by affecting the core microbial community during distilled grain waste composting. Biores Technol 337:125492. https://doi.org/10.1016/j.biortech.2021.125492

Willems DJ, Kumar A, Nugegoda D (2023) Mixture toxicity of three unconventional gas Fracking Chemicals, Barium, O-Cresol, and Sodium Chloride, to the freshwater shrimp Paratya australiensis. Environ Toxicol Chem 42(2):481–494. https://doi.org/10.1002/etc.5538

Yang X, Li J, Liang T, Yan X, Zhong L, Shao J, El-Naggar A, Guan GY, Liu J, Zhou Y (2021) A combined management scheme to simultaneously mitigate as and cd concentrations in rice cultivated in contaminated paddy soil. J Hazard Mater 416:125837. https://doi.org/10.1016/j.jhazmat.2021.125837

Yi Z, Li C, Li Q, Zhang L, Zhang S, Wang S, Qin L, Hu X (2022) Influence of CO2 atmosphere on property of biochar from pyrolysis of cellulose. J Environ Chem Eng 10(3):107339. https://doi.org/10.1016/j.jece.2022.107339

Yoon GS, Park SM, Yang H, Tsang DCW, Alessi DS, Baek K (2018) Selection criteria for oxidation method in total organic carbon measurement. Chemosphere 199:453–458. https://doi.org/10.1016/J.CHEMOSPHERE.2018.02.074

Younis SA, El-Salamony RA, Tsang YF, Kim KH (2020) Use of rice straw-based biochar for batch sorption of barium/strontium from saline water: Protection against scale formation in petroleum/desalination industries. J Clean Prod 250:119442. https://doi.org/10.1016/J.JCLEPRO.2019.119442

Yuan JH, Xu RK, Zhang H (2011) The forms of alkalis in the biochar produced from crop residues at different temperatures. Bioresour Technol 102:3488–3497. https://doi.org/10.1016/J.BIORTECH.2010.11.018

Yuan Y, Bolan N, Prévoteau A, Vithanage M, Biswas JK, Ok YS, Wang H (2017) Applications of biochar in redox-mediated reactions. Bioresour Technol 246:271–281. https://doi.org/10.1016/j.biortech.2017.06.154

Yuan P, Wang J, Pan Y, Shen B, Wu C (2019) Review of biochar for the management of contaminated soil: Preparation, application and prospect. Sci Total Environ 659:473–490. https://doi.org/10.1016/J.SCITOTENV.2018.12.400

Yun D, Cho E, Dindulkar SD, Jung S (2016) Succinoglycan Octasaccharide Conjugated polydiacetylene-doped Alginate beads for Barium (II) detection. Macromol Mater Eng 301:805–811. https://doi.org/10.1002/MAME.201600060

Zama EF, Zhu YG, Reid BJ, Sun GX (2017) The role of biochar properties in influencing the sorption and desorption of pb(II), cd(II) and as(III) in aqueous solution. J Clean Prod 148:127–136. https://doi.org/10.1016/j.jclepro.2017.01.125

Zhang H, Chen C, Gray EM, Boyd SE (2017) Effect of feedstock and pyrolysis temperature on properties of biochar governing end use efficacy. Biomass Bioenergy 105:136–146. https://doi.org/10.1016/J.BIOMBIOE.2017.06.024

Zhao SX, Ta N, Wang XD (2017) Effect of temperature on the structural and physicochemical properties of biochar with Apple tree branches as feedstock material. Energies 10(9):1293. https://doi.org/10.3390/EN10091293

Zuhara S, McKay G (2024) Waste-derived activated carbons for effective adsorptive removal of strontium, barium, and binary pollutants: a response surface methodology study. J Environ Chem Eng. https://doi.org/10.1016/j.jece.2024.112836